Structural Change of Site-Directed Mutants of PYP: New Dynamics during pR State

Kan Takeshita,* Yasushi Imamoto,† Mikio Kataoka,† Ken'ichi Mihara,† Fumio Tokunaga,‡ and Masahide Terazima*

*Department of Chemistry, Graduate School of Science, Kyoto University, Kyoto 606-8502, Japan; †Graduate School of Materials Science, Nara Institute of Science and Technology (NAIST), Nara 630-0101, Japan; and ‡Department of Earth and Space Science, Graduate School of Science, Osaka University, Toyonaka, Osaka 560-0043, Japan

ABSTRACT The energetics, protein dynamics, and diffusion coefficients of three mutants of photoactive yellow protein, R52Q, P68A, and W119G, were studied by the transient grating and pulsed laser-induced photoacoustic method. We observed a new dynamics with a lifetime of ~1 μs in the transient grating signal, which is silent by the light absorption technique. This fact indicates that, after the structure change around the chromophore is completed (pR_1), the protein part located far from the chromophore is still moving to finally create another pR (pR_2) species, which can transform to the next intermediate, pB. Although the kinetics of $pR_2 \rightarrow pB \rightarrow pG$ are very different depending on the mutants, the enthalpies of the first long-lived (in microseconds, 100-μs range) intermediate species (pR_2) are similar and very high for all mutants. The diffusion coefficients of the parent (pG) and pB species of the mutants are also similar to that of the wild-type photoactive yellow protein. From the temperature dependence of the volume change, the difference in the thermal expansion coefficients taken as indicator of the flexibility of the structure between pG and pR_2 is measured. They are also similar to that of the wild-type photoactive yellow protein. These results suggest that the protein structures of pR_2 and pB in these mutants are globally different from that of pG, and this structural change is not altered so much by the single amino acid residue mutation. This is consistent with the partially unfolded nature of these intermediate species. On the other hand, the volume changes during $pR_1 \rightarrow pR_2$ are sensitive to the mutations, which may suggest that the volume change reflects a rather local character of the structure, such as the chromophore-protein interaction.

INTRODUCTION

Photoactive yellow protein (PYP), first isolated from the purple sulfur bacterium *Ectothiorhodospira halophila* (Meyer, 1985) and later also found in other purple bacteria (Koh et al. 1996), is a 14-kDa cytosolic photoreceptor controlling negative phototaxis response. Unlike the well-known light receptors rhodopsin, bacteriorhodopsin, and sensory rhodopsin, all of which are integral membrane proteins, PYP is water-soluble and its chromophore is *p*-hydroxycinnamyl bound via a thioester bond to Cys-69 (Baca et al., 1994; Hoff et al., 1994a). The three-dimensional structure, refined at 1.4-Å resolution, indicates that PYP contains a central β-sheet flanked on each side by short loops and helices (Borgstohl et al., 1995). Because the high-resolution crystal structure information is available, PYP has been receiving increasing attention as a model protein for photo-signal transduction.

The photocyclic reaction of PYP has been studied mainly by flash photolysis techniques using the optical transition of the chromophore. Picosecond transient absorption spectroscopy (Ujj et al., 1998; Devanathan et al., 1999) revealed that the first intermediate (I_0) appears in <3 ps after 452-nm excitation of PYP. Kinetic analysis showed that I_0 decays with a 220-ps lifetime, leading another intermediate ($I_0^{\neq}$) with a similar absorption spectrum as I_0. $I_0^{\neq}$ decays with a 3-ns lifetime to form a rather stable intermediate, pR, and it is converted to a new species, pB, with a double exponential kinetics in hundreds microseconds. (Sometimes, pR and pB are expressed by I_1 and I_2, respectively. Here we will use the pR and pB notations.) Finally, pB is converted back to the original (parent) species (pG) in hundreds of milliseconds.

The structure of pB has also been solved to 1.9 Å by millisecond time-resolved Laue crystallography (Genick et al., 1997a). The results show that light-induced conformational changes are confined to the region of the chromophore and involve *trans-cis* photoisomerization of the *p*-hydroxycinnamyl double bond and movement of a small number of nearby amino acid residues. From these data, the protein structure change in pR should be localized around the chromophore. However, the thermodynamic measurements (Van Brederode et al., 1996; Ohishi et al., 2001), nuclear magnetic resonance studies (Düx et al., 1998; Rubinstenn et al., 1998; Craven et al., 2000), and infrared spectroscopy (Kandori et al., 2000; Xie et al., 2001; Brudler et al., 2001) suggest a more global change in the protein structure of pB in solution.

In our previous papers, we reported the enthalpy (ΔH) and the volume changes (ΔV) for the pG→pR process and diffusion coefficients of pG and pB for the wild-type (WT) PYP (Takeshita et al., 2000, 2002). We found a large temperature dependence of the volume change associated with this process. The volume change was -7 cm^3/mol at 20°C, and the absolute value increases with decreasing the

Submitted January 28, 2002, and accepted for publication May 17, 2002.

Address reprint requests to Masahide Terazima, Department of Chemistry, Graduate School of Science, Kyoto University, Kyoto 606-8502, Japan. Tel.: 81-75-753-4026; Fax: 81-75-753-4000; E-mail: mterazima@kuchem.kyoto-u.ac.jp.

0006-3495/02/09/1567/11 $2.00

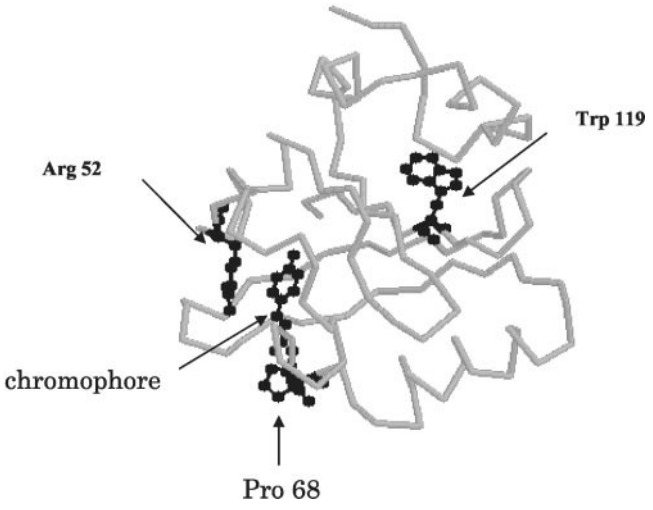

FIGURE 1 The structure of WT-PYP. The amino acid residues replaced in this study are highlighted.

temperature: -15 cm^3/mol at 0°C. This temperature dependence of the volume change was interpreted as arising from that the thermal expansion coefficient (α) of pR is much larger than that of pG. The observed negative volume change and the difference in the thermal expansion coefficient between pG and pR ($\Delta\alpha$) were interpreted in terms of the loosened protein structure in the pR state. Furthermore, the diffusion coefficients (D) of pG and pB were determined, and it was found that D of pG is $\sim$1.2 times larger than that of pB. The smaller D of pB was discussed in terms of the compact factor and the roughness of proteins and these considerations supported the suggestion that the reaction intermediates, pR and pB, have partially unfolded (loosened) protein structures.

In the present study, we investigate the structural dynamics as well as the enthalpy changes of some mutants of PYP to obtain further information of the dynamics but rather the structures. If the structural change in pR is not restricted to the surroundings of the chromophore and the whole protein structure is loosened as previously suggested, any one residue mutation would not change the essential features of $\Delta\alpha$ or D as long as the photocycle reaction takes place. Here we used three mutants, R52Q, P68A, and W119G (Fig. 1) because of the following reasons. The location of Arg-52 suggests that it separates the active site from the solvent in the ground state and stabilizes the negative charge on the chromophore by providing the opposite electrostatic charge. The volume and enthalpy changes of R52Q should thus provide information on whether this electrostatic stabilization is important for these properties or not. In most of PYPs, Pro is reserved at the next residue to the chromophore site. The presence of this residue could be important for the structure and the function. These two amino acids are located near the chromophore site. On the other hand, Trp-119 is located at a rather far distance from the chromophore site. Comparison of the other mutants with W119G may give us a clue for a question: how important is a residue distant from the chromophore site. Although the rate constant of the reaction is altered depending on the mutant, all mutants show a photocycle as the WT-PYP, and all these mutations do not change the ground state absorption spectra too much. This further result indicates that the microenvironment around the chromophore does not change. These properties are suitable to study the role of the protein part of PYP.

We found that $\Delta\alpha$ of these mutants as well as WT-PYP are very similar to each other, and this fact supports the global change of the protein structure by the photocyclic reaction because only one residue mutation is not expected to change the loosened structure of the protein. Furthermore, the D values of pG and pB of these mutants are compared with those of WT-PYP, and this comparison also indicates that the compact factor is not changed by the mutation. Interestingly, on microsecond time scale, we observed a new dynamics that has never been detected by the other spectroscopic methods so far. Because on this time scale pR is already created, this new dynamics indicates that parts of the protein far from the chromophore are still moving after the pR state is created. Therefore, the pR state is not a single state, but subsequent change of the protein structure that does not affect the chromophore's absorption (probably it is located distant from the chromophore) is essential to finally prepare pR leading pB; that is, the protein structure that changes the chromophore's conjugated system or the hydrogen bonding network around the chromophore is initially changed within 3 ns and then the other protein part moves with a microsecond lifetime. This dynamics depends on the mutation. This observation may be the most direct evidence for the global change of the protein in pR. Based on this result, the two pR species with different structures distant from the chromophore site are called pR_1 and pR_2.

PRINCIPLE

The detail of the transient grating (TG) method has been reported previously (Terazima, 1998). Under a weak diffraction condition, the intensity of the TG signal ($I_{TG}(t)$) is given by

$$I_{TG}(t) = \alpha'(\delta n(t))^2 + \beta'(\delta k(t))^2 \qquad (1)$$

in which α' and β' are constants, and $\delta n(t)$ and $\delta k(t)$ are the peak-null difference of the refractive index and the absorbance, respectively. In this PYP case, because the absorption at the probe wavelength is negligible, the TG signal intensity is proportional to the square of $\delta n(t)$. There are two main contributions to the refractive index change: the thermal effect and a change of chemical species by the reaction.

We represent the former as $\delta n_{th}(t)$ (thermal grating), the latter as $\delta n_{spe}(t)$ (species grating).

$$I_{TG}(t) = \alpha'\{\delta n_{th}(t) + \delta n_{spe}(t)\}^2 \quad (2)$$

Because the amplitudes of the spatial modulation of the thermal grating and the species grating, respectively, decrease by thermal diffusion and molecular diffusion processes, the time dependence can be expressed by Eq. 3.

$$\delta n_{th}(t) = \delta n^0_{th}(t)*\exp(-D_{th}q^2t)$$

$$\delta n_{spe}(t) = \delta n^{i0}_{spe}(t)*\exp(-D_iq^2t) \quad (3)$$

in which * represents the convolution integral, D_{th} is the thermal diffusivity, D_i is the diffusion coefficient of species i, and q is the grating wavenumber given by $q = \pi \sin(\theta/2)/\lambda_{ex}$ (λ_{ex} is wavelength of the excitation light). We can vary q by varying the crossing angle (θ) between two excitation beams. δn^0_{th} and δn^{i0}_{spe} are intrinsic refractive index changes caused by the released heat from the excited state and creation (or extinction) of species i, respectively. Because D_{th} is usually one or two orders of magnitude larger than D_i in solution, the thermal component can be easily separated from the species grating signal.

The amplitude of the thermal grating (δn_{th}) is the refractive index change due to temperature change given by Eq. 4.

$$\delta n_{th} = \frac{dn}{dT}\Delta T = \frac{dn}{dT}\frac{OW}{\rho C_p}\Delta N \quad (4)$$

in which dn/dT is the refractive index change with temperature, ΔT is the temperature change, W is the molecular weight (g/mol), ρ is the density (g/cm^3) of the solvent, ΔN the molar density of the excited molecule (mol/cm^3), and Q is the released thermal energy (J/mol). We determine Q by comparison with δn_{th} of a calorimetric reference sample, which converts all the absorbed photon energy to the thermal energy.

There are two contributions to δn^i_{spe}; the refractive index change due to the change in the absorption spectrum (population grating; δn^i_{pop}) and by the molecular volume change (volume grating; δn^i_{vol}). The magnitude of the volume grating (δn_{vol}) is given by

$$\delta n_{vol} = V\frac{dn}{dV}\Delta V\Delta N \quad (5)$$

in which $V(dn/dV)$ is the refractive index change due to the molecular volume change, and ΔN is the number of the reacting molecules in a unit volume. Therefore, we can determine the absolute value of ΔV after a quantitative measurement of δn_{vol} and knowing the solvent property ($V(dn/dV)$).

EXPERIMENTAL

The detailed experimental setup for the TG (Terazima and Hirota, 1993) experiments was already reported. In this study, a XeCl excimer laser-pumped dye laser (Lamda Physik Compex 102xc, Göttingen, Germany, Lumonics Hyper Dye 300; λ = 465 nm) was split into two by a beam splitter and crossed inside a quartz sample cell (optical path-length = 2 mm). The laser power of the excitation was <5 μJ/pulse. The created interference pattern (transient grating) in the sample was probed by a He-Ne laser (633 nm) or a diode laser (840 nm) as a Bragg diffracted signal (TG signal). The TG signal was detected by a photomultiplier tube (Hamamatzu R-928, Iwata, Japan) and fed into a digital oscilloscope (Tektronix 2430A, Tokyo, Japan). The TG signal was averaged by a microcomputer to improve the signal to noise ratio.

The repetition rate of the excitation laser was ~0.5 to ~0.2 Hz. This repetition rate is, in particular at low temperatures, faster than the lifetimes of pB. However, in this paper, we focus our attention in a time range of 0 to 100 ms, because the final decay rate of the TG signal is determined by the molecular diffusion process, which is faster than the intrinsic reaction rate as described later. Therefore, the slowest return rate to pG is not important in this measurement. Furthermore, because the pump light (less than 5 μJ/pulse) excites less than 10% of PYP in the illuminated region and the excitation is spatially inhomogeneous for the TG measurement, the photoexcited PYP molecule should be relaxed or diffused away before the next excitation pulse comes in. Hence, we can neglect a possible multiple excitation of PYP at any temperature. We confirmed that decreasing the repetition rate further did not change the observed TG signal within our experimental uncertainty.

Three mutants of PYP, i.e., R52Q, P68A, and W119G, were prepared by the site-directed mutagenesis technique as reported previously (Mihara et al. 1997; Imamoto et al., 2001a). The purity of the samples was checked by "the purity index values" (the ratio of the absorbance at 275 nm to that at 446 nm) and they were 0.46 for R52Q, 0.47 for P68A, and 0.36 for W119G (data not shown). The absorption coefficient of pG at 446 nm were measured by a method reported previously (Imamoto et al., 2001a). These mutants of PYP was dissolved in 10 mM Tris-HCl (pH 8.0) with 1 mM PMSF (phenylmethanesulfonyl fluoride). BCP (bromocresol purple) was used as a calorimetric reference (Braslavsky and Heibel, 1992). Concentration of the sample in the buffer and the reference molecule in aqueous solution were adjusted so that the absorbance in the cell was the same at the excitation wavelength. The thermodynamical properties of the buffer such as dn/dT was confirmed to be the same as the aqueous solution within our experimental uncertainty ($\pm$5%) by a comparison of the thermal grating signal intensities from the calorimetric samples in these solvents with the same absorbance under the same condition. Absorbance was ~0.5 to ~1.0 in each experiment.

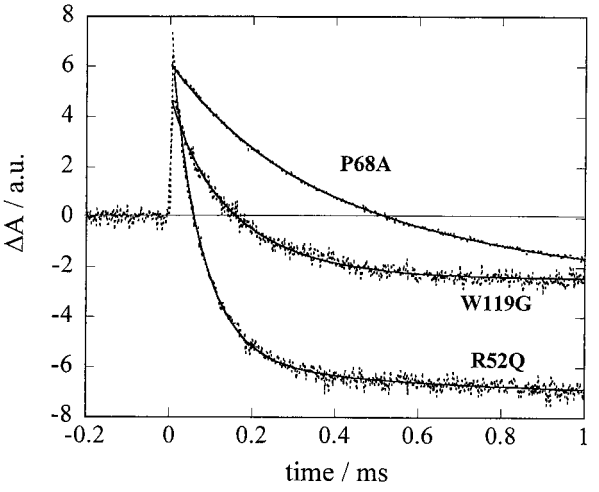

FIGURE 2 Time profiles of transient absorption signals (ΔA) of R52Q, P68A, and W119G in 10 mM Tris-HCl buffer with 1mM phenylmethanesulfonyl fluoride after photoexcitation at 465 nm, monitored at 488 nm (dotted line). The best fitted curves by Eq. 6 are shown by the solid lines.

RESULTS

Absorption spectra

Before describing the TG results, we briefly present the steady state and time-resolved absorption spectra of these mutants. The ground state absorption spectra of the mutants are not much different from that of WT-PYP. The absorption maxima of WT-PYP, R52Q, P68A, and W119G are 446, 447, 446, and 445 nm, respectively. The very small shifts of the spectra indicate that the replacement of these amino acids do not change much the microenvironment properties around the chromophore. The substitution effect on the kinetics of the photocycle and the intermediate species were investigated by flash photolysis. The time profiles monitored at 488 nm and the transient absorption (TA) spectra at 1 μs and 1 ms after photoexcitation are shown in Fig. 2 and 3, respectively. The TA spectrum of each mutant is similar to that of WT-PYP. Therefore, the structures around the chromophore not only in the ground state but also in the pR and pB states are similar to that of WT-PYP.

The qualitative features of the kinetics monitored by the TA signal after photoexcitation of the mutants are also similar to that of WT-PYP. The kinetics ($I_{TA}(t)$) can be expressed by a four-exponential function:

$$I_{TA}(t) = a_1\exp(-t/\tau_1) + a_2\exp(-t/\tau_2) + a_3\exp(-t/\tau_3) + a_4\exp(-t/\tau_4) \quad (6)$$

in which τ_i are the lifetimes. The two terms (τ_1 and τ_2) of the right hand side represent the lifetimes of the pR→pB process and the other (τ_3 and τ_4) are assigned to the pB→pG process. The lifetimes of pR→pB and pB→pG are changed considerably by the mutation. For all the mutants we investigated, the pR→pB process is accelerated compared with the WT-PYP, whereas the pB→pG process is slowed down by the mutations. Because we focus our attention on the

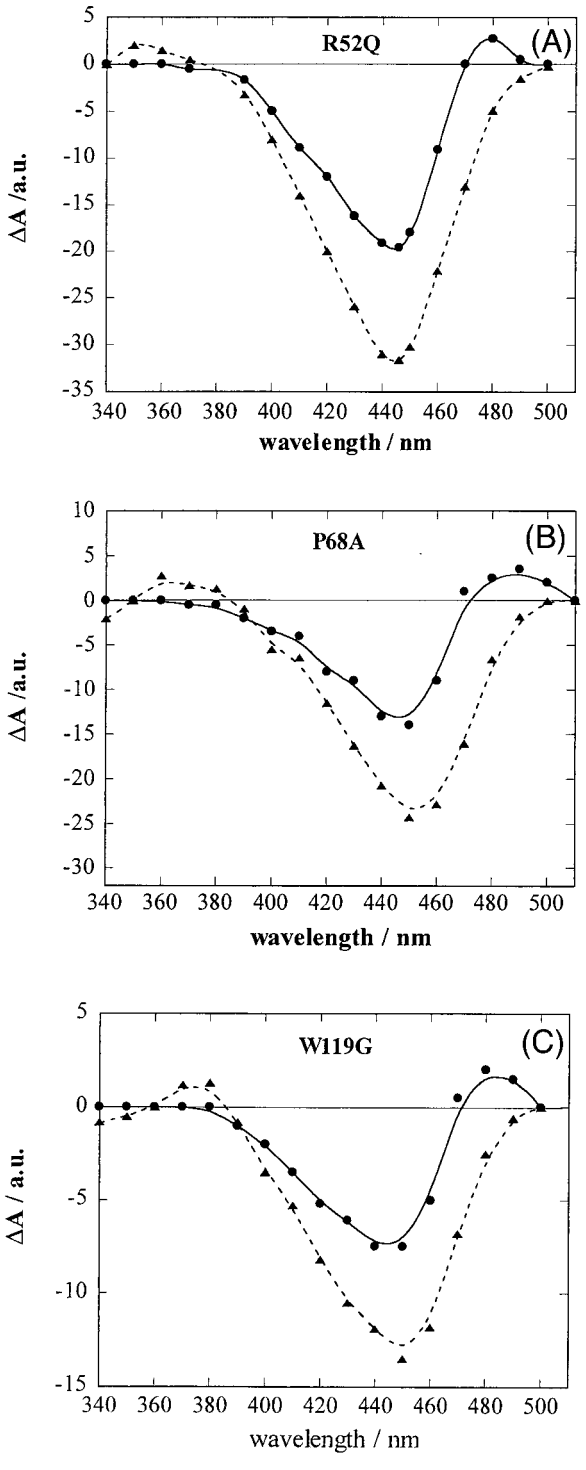

FIGURE 3 Transient absorption spectra of PYP mutants R52Q, P68A, and W119G after photoexcitation at 465 nm. The difference of the absorption (ΔA) between pG and the intermediate species pR monitored 1 μs after excitation (circles), and between pG and pB 1 ms after excitation (triangles). The lines are guide for the eyes.

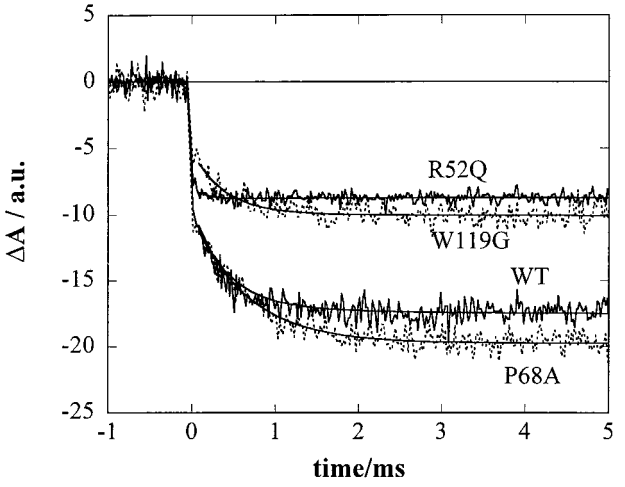

FIGURE 4 Temporal dependence of the photobleaching signal monitored at 446 nm concomitant with the pB formation of three mutants and WT. The signal intensity reflects the photo-depletion of PYP by photoexcitation. The smooth solid lines are fitted curves by Eq. 6.

dynamics of pR→pB and we will not consider the decay kinetics here, we list only the lifetimes of the pR→pB process in Table 1.

The relative quantum yields of the photocyclic reaction of the mutants were measured by comparing the TA intensity at 5 ms after photoexcitation at 446 nm. Fig. 4 depicts the photobleach signals concomitant with the pR→pB process of WT-PYP and the mutants under the same experimental conditions. Assuming that pB has no absorption at 446 nm, the TA signal intensity (I_{TA}(446 nm)) is given by

$$I_{TA}(446\ \text{nm}) = AI\Phi\varepsilon_{446} \qquad (7)$$

in which A is a constant, I is the excitation light intensity, and ϵ_{446} is the absorption coefficient of pG at 446 nm. Using $\epsilon_{446} = 4.55 \times 10^4$, 4.2×10^4, 4.46×10^4, and 4.47×10^4 for WT, R52Q, P68A, and W119G, respectively, and $\Phi = 0.35$ for WT-PYP, we determined Φ of three mutants and listed in Table 2.

The temperature dependence of Φ was measured through the TA signal intensity. For all mutants, Φ is not so sensitive to temperature in a range 20°C to 10°C, but it decreases with decreasing the temperature below 10°C (Fig. 5). This

TABLE 1 Decay rates of pR → pB of each mutant measured by transient absorption at 20°C

	pR → pB (intensity ratio)
WT	170 μs, 1 ms (1:2)
R52Q	75 μs, 400 μs (5:1)
P68A	150 μs, 400 μs (1:1)
W119G	150 μs

The relative intensities of two components for pR → pB are shown in parenthesis.

TABLE 2 Photoreaction quantum yields (Φ) of WT and the mutants of PYP at 20°C measured by the transient absorption signal

WT	0.35 (Van Brederode el al., 1995)
R52Q	0.21 ± 0.08
P68A	0.42 ± 0.08
W119G	0.21 ± 0.08

is similar to what we already reported for WT-PYP (Takeshita et al., 2000, 2002).

TG signals

Fig. 6 depicts the temporal profiles of the TG signals after photoexcitation of R52Q, P68A, and W119G. The TG signals in an early time range are presented in linear time scale in the insets. The qualitative features, the fitting procedure, and the assignment of the signal components in the TG signal have already been presented for WT-PYP (Takeshita et al., 2000, 2002).

The features and the assignments are briefly described as follows for a comparison with the signal of the mutants (Takeshita et al., 2002). Initially the signal rises quickly after photoexcitation with the instrumental response of our system and then shows a weak slow rising component. After this, the signal decays to a certain intensity with a time constant $D_{th}q^2$, and shows growth-decay curves twice during the observation time. Because there is no absorption by the parent and the intermediate species at the probe wavelength, the observed TG signal should be explained by the photoinduced refractive index change. The component that decays with $D_{th}q^2$ should be the thermal grating component and the latest growth-decay curve was attributed to the

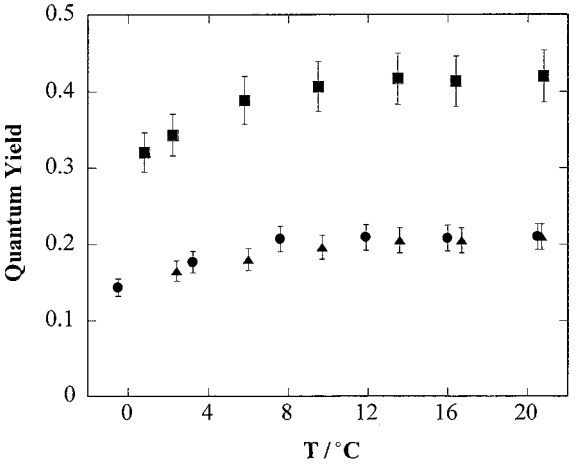

FIGURE 5 Temperature dependence of quantum yields of the photoreaction for three mutants; R52Q (circles), P68A (squares), and W119G (triangles) monitored from the transient photobleach signals monitored at 446 nm.

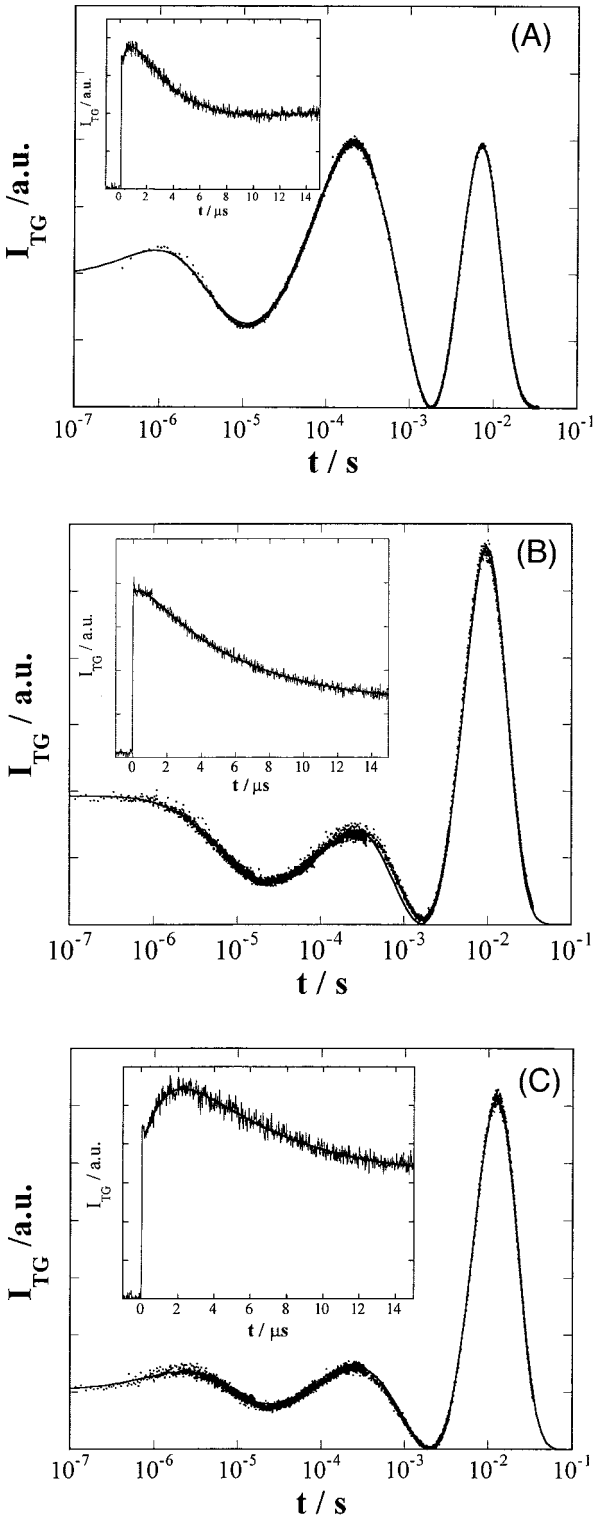

FIGURE 6 The TG signals of PYP mutants (A) R52Q, (B) P68A, and (C) W119G after photoexcitation at 465 nm and monitored at 633 nm. The insets show the TG signals in the short time range. Smooth solid lines are the best fitted curves by Eq. 8.

protein diffusion process of pG and pB (Takeshita et al., 2000, 2002).

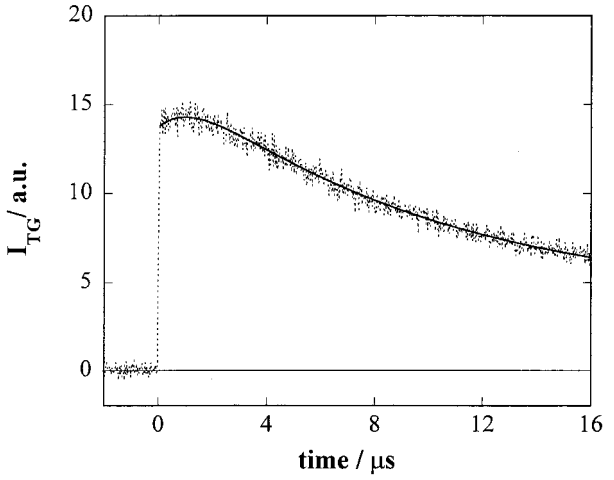

FIGURE 7 TG signal for WT-PYP (dotted line) at a small grating vector q ($q = 7.4 \times 10^5$ m^{-1}). The best fitted line by Eq. 8 is shown by the solid line.

We found that the TG signal in the whole time range can be well expressed by

$$I_{TG}(t) = \alpha'\{a_f\exp(-t/\tau_f) + a_s\exp(-t/\tau_s) + a_{th}\exp(-t/\tau_{th}) + a_1\exp(-t/\tau_1) + a_2\exp(-t/\tau_2) + a_{pG}\exp(-D_{pG}q^2t) + a_{pB}\exp(-D_{pB}q^2t)\}^2 \quad (8)$$

in which τ_f is the lifetime of the fast rising component, which is determined by the instrumental response ($\tau_f \sim 10$ ns), τ_s is the lifetime of the slow rising component as described in the next section in detail, D_{pG} and D_{pB} are the diffusion coefficients of pG and pB, respectively. The lifetimes τ_1 and τ_2 represent the pR→pB kinetics as defined in Eq. 6. The TG signals of all mutants examined here can be analyzed with this equation.

Dynamics far from the chromophore

One of novel observations in this present work is the slow TG rising component on a microsecond time scale. Previously this component was not discussed in detail because the intensity was very weak for WT-PYP, and the separation of this component from the thermal diffusion component was difficult. However, a careful examination definitively indicates the presence of this component. This rising component is much easier to observe under a small q condition (Fig. 7), because the decay of the thermal grating under this condition becomes slow and the time constant τ_s and $(D_{th}q^2)^{-1}$ become very different. This slow rising component is relatively large for R52Q and W119G but is weak for WT and P68A. In this section, we examine the nature of this component.

Fig. 8 shows the temperature dependence of the initial part of the thermal grating for R52Q. There are several

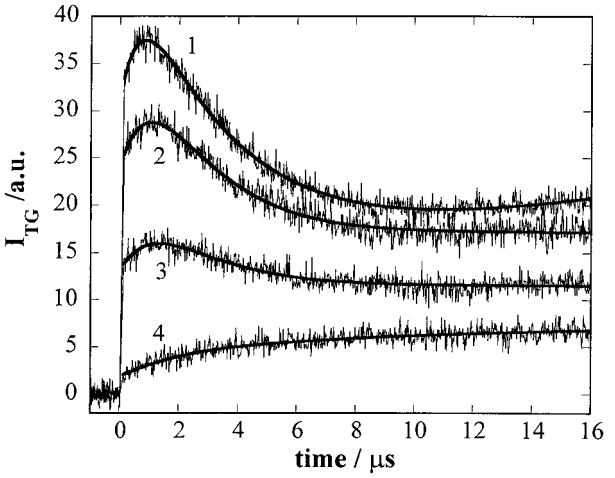

FIGURE 8 TG signals for R52Q at various temperatures after photoexcitation at 465 nm, monitored at 633 nm. Temperatures are for 20.4, 16.1, 11.7, and 2.2°C for traces 1–4, respectively. Smooth solid lines are the best fitted curves by Eq. 8.

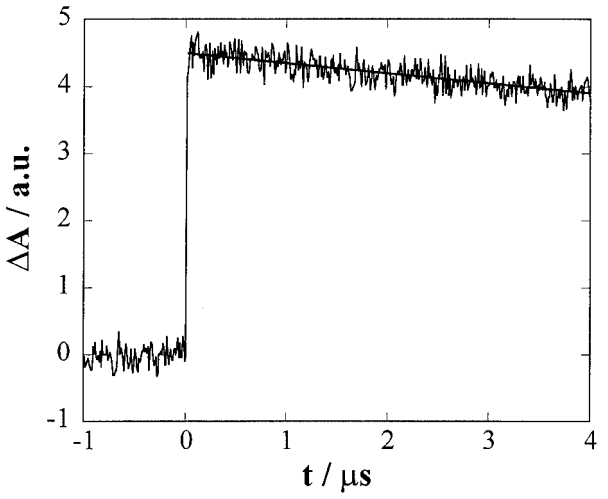

FIGURE 9 Temporal dependence of the transient absorption signal (ΔA) of R52Q after photoexcitation at 465 nm, probed at 488 nm. The smooth curve is the fitted line with lifetimes of 75 μs and 400 μs. Compared with the time profile of the TG signal (Fig. 6(A)), it is apparent that there is no kinetic component on this time scale.

points we should note. First, with decreasing temperature, the thermal grating signal intensity becomes weaker. This temperature dependence of the thermal grating signal intensity is explained by the temperature dependence of $|dn/dT|$ (Eq. 4), which decreases with decreasing the temperature until 0°C. Second, the intensity, i.e., the preexponential factor a_s, does not depend on the temperature so much, (although the fitting is less accurate because of the weak intensity of this component). Even close to 0°C (2.2°C, curve 4 in Fig. 8), where the thermal contribution can be almost neglected, we can observe this slow rising. Therefore, the main part of the slow rising component is not due to the thermal contribution, but it should be due to either population grating and/or volume grating contribution.

In the time profile of the TA signal, this dynamics is not present as shown in Fig. 9 and also a number of reports on the PYP dynamics studied by the flash photolysis method have never observed this dynamics at any visible wavelengths (Hoff et al., 1994b; Ujj et al., 1998; Devanathan et al., 1999). Hence, this is an optically silent dynamics. It is reasonable to attribute this component to the volume grating term or the population grating due to the absorption change in a far ultraviolet region (Eq. 2). Regardless of the exact assignment, the presence of this dynamics in the TG signal indicates that there is an intermediate species between the creation of the usually referred pR and pB states. In this paper, the two species in pR are called pR_1 and pR_2. Hence the reaction scheme of PYP should be described as shown in Scheme 1. (It may possible that pR_1 and pR_2 species are in equilibrium with the lifetime of 1 μs. However, we cannot distinguish whether the transition of pR_1 to pR_2 is irreversible or reversible from the present experiment. Here we tentatively assume that the transition is irreversible.)

In particular, we should again stress that this dynamics observed in the grating signal cannot be observed in the visible absorption signal of the chromophore. This fact indicates that the structural change that appears in the grating signal is a conformational change distant from the chromophore site. Although the protein structure that affects the absorption spectrum of the chromophore is initially changed within 3 ns upon creation of pR_1, the other protein parts move with a microsecond lifetime. This observation may be the most direct evidence for a global change of the protein in pR. If this rising component comes from the volume change entirely, the volume change (ΔV) in this

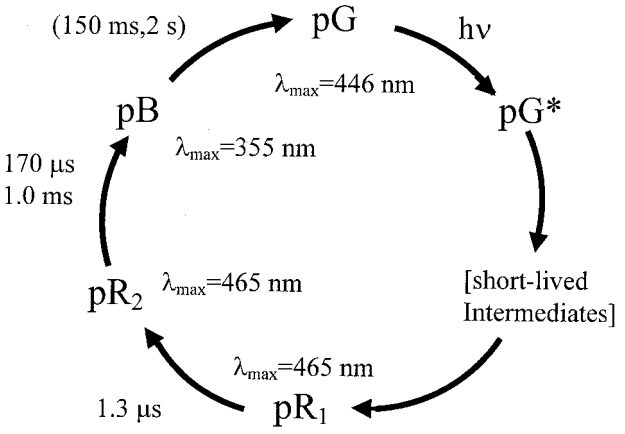

SCHEME 1 Revised photoreaction cycle of WT-PYP at room temperature after 10 ns of photoexcitation. Wavelengths at peaks of the absorption spectra and the lifetimes at 20°C are also shown. The longest lifetimes (150 ms, 2 s) were not measured in the present study but taken from literature (Hoff, 1994b).

TABLE 3 Lifetimes (τ_s) of the $pR_1 \rightarrow pR_2$ process of WT and three mutants of PYP and the volume changes (ΔV) associated with this process by assuming that the entire slow rising TG signal comes from the volume grating component

	$\tau_s/\mu s$	$\Delta V(pR_1 \rightarrow pR_2)$/ $cm^3\ mol^{-1}$	ΔH/kJ mol^{-1}	$\Delta\alpha/cm^3\ mol^{-1}\ K^{-1}$
WT	1.3 ± 0.4	5 ± 1	160 ± 15	+0.6
R52Q	0.7 ± 0.2	15 ± 2	185 ± 30	+0.5
P68A	0.6 ± 0.4	3 ± 1	120 ± 20	+0.4
W119G	1.3 ± 0.2	23 ± 3	230 ± 40	+0.7

ΔH of pR_2 and $\Delta\alpha$ for the $pG \rightarrow pR_2$ process of WT and three mutants are also listed. ΔH are determined from the thermal grating signal intensities, and $\Delta\alpha$ are calculated from the temperature dependence of the volume grating intensity.

dynamics can be calculated from the intensity of this component using Eq. 5. ΔV are +5 cm^3/mol, +15 cm^3/mol, +3 cm^3/mol, and +23 cm^3/mol for WT, R52Q, P68A, and W119G, respectively (Table 3). This result indicates that the dynamics far from the chromophore depends on the mutation.

ΔH of pR_2

The thermal grating signal intensity represents the thermal energy released by the nonradiative transition during the $pG \rightarrow pR_2$ process. Hence, the enthalpy of the pR_2 state can be determined from the measurement of the absolute signal intensity. This is one of the advantages of the TG technique compared with the other techniques. For the quantitative measurement, we compared the signal intensities of the PYP samples with that of the calorimetric reference sample. We used BCP (bromocresol purple) as the calorimetric reference because all of the photon energy absorbed by BCP is released as heat with a quantum yield of unity (Braslavsky and Heibel, 1992). Using this reference probing at 633 nm and Eq. 4, $\Phi\Delta H$ for the WT and the mutant of P68A are determined. For R52Q and W119G, the grating signal beneath the thermal grating (the population and volume grating components) is relatively large, and an accurate separation of the thermal grating signal from the other contributions was difficult by the probing at 633 nm. To improve the accuracy, we probed the TG signal at 840 nm because the probe wavelength shift to a further red side of the main absorption band of PYP reduces the relative contribution of the population-grating signal and the fitting was much easier. Using the quantum yield of the reaction, Φ, of the WT and mutants, ΔH was determined (Table 3).

Temperature dependence of volume change

In our previous papers, we described the first observation of the temperature dependent volume change of pR_2 (Takeshita et al., 2000, 2002). This temperature dependence of the volume change is interpreted as arising from the different thermal expansion coefficient ($\Delta\alpha$) of pG and pR_2. This was taken as evidence to support the flexible protein structure in pR_2. We examined the temperature dependence of ΔV for the mutants using the temperature dependence of the volume grating intensity as reported previously (Takeshita et al., 2000, 2002). The grating signal beneath the thermal grating signal is a sum of the population and volume grating contributions. Because the TA signal intensity does not depend on the temperature besides the temperature-dependent Φ, the temperature-dependent part of the grating signal beneath the thermal grating should represent the volume grating contribution. Therefore, ΔV is calculated from the volume grating intensity by taking into account the temperature-dependent Φ. The results are shown in Fig. 10.

Diffusion coefficients of pG and pB

The latest growth-decay curve of the TG signal (Fig. 6) represents the diffusion processes of pG and pB in the solution (the sixth and seventh terms in the right side of Eq. 8). As described in the previous paper, the assignment of the diffusing species was made from the sign of the refractive index change (Takeshita et al., 2002). The rate constant of the rising component represents $D_{pG}q^2$ and that of the decaying component corresponds to $D_{pB}q^2$. By fitting the signal at different q, D_{pG}, and D_{pB} are determined. We found that D_{pG} and D_{pB} of the mutants are almost the same as those of WT-PYP ($D_{pG} = 1.2 \pm 0.1 \times 10^{-10}$ m^2/s, and $D_{pB} = 1.0 \pm 0.1 \times 10^{-10}$ m^2/s).

DISCUSSION

Mutation effect on the kinetics

Genick et al. (1997b) have studied the effect on the photocycle kinetics of several PYP mutations such as E46Q and R52A and pH dependence. They observed that pR→pB is accelerated by these mutations and that the pB→pG process becomes faster and slower on E46Q and R52A mutations, respectively. The pR→pB transition involves the displacement of Arg-52 from its original position and the exposure of the chromophore to the solvent. This leads to a proton uptake by the chromophore. Based on this model, they have explained the acceleration of the pR→pB process by the mutation so that the truncation of Arg-52 opens the way for the chromophore without having to displace the arginine side chain. Furthermore, it is now suggested that Arg-52 helps to stabilize the negative charge on the chromophore by providing the opposite electrostatic charge. Changing this residue to such as Gln accelerates the protonation of the chromophore and stabilizes this state (pB). Hence, R52Q is expected to accelerate the pR→pB process but to slow down the pB→pG process. Our kinetics result on R52Q is consistent with this interpretation and expectation. How-

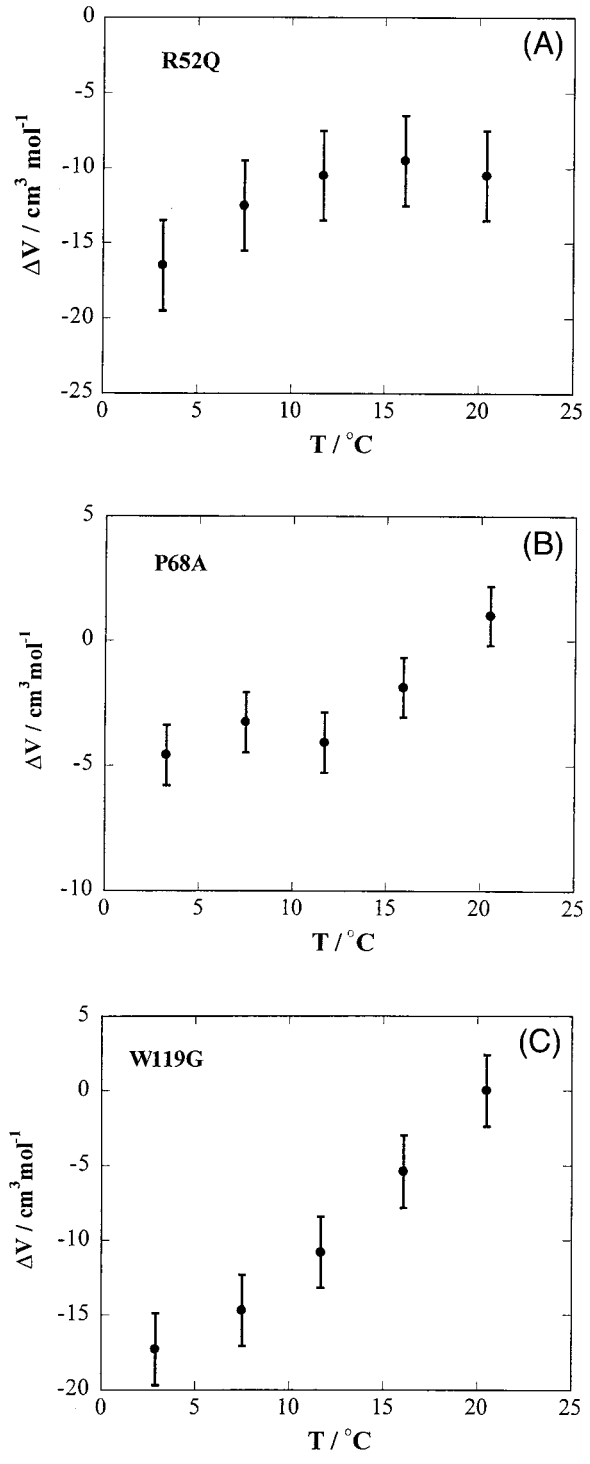

FIGURE 10 Temperature dependent volume changes of three mutants determined from the intensity of the volume grating.

ever, not only R52Q, the other mutants, P68A and W119G, also show a similar trend, even though the effect is less conspicuous. It is particularly interesting to note that even replacing Trp-119 that is located at a rather far distance from the chromophore site affects the kinetics. Therefore, the overall protein conformation is also important to determine the kinetics of the reaction.

The enthalpy difference between pG and pR_2 is high for all mutants and for WT-PYP. Although the entropy could be an important factor to control the reaction from pR_2 to pB, the observed large ΔH suggests that the main origin of the driving force for the $pR_2 \rightarrow pB$ reaction may be this large enthalpy change. However, we could not find a clear correlation between ΔH and Φ. This negligible correlation may indicate that the quantum yield of the reaction is determined by the initial step of the photoisomerization on much faster time scale; that is, the quantum yield of the reaction is determined by the quantum yield of the *trans-cis* isomerization of the chromophore. Once the photoisomerization of the chromophore takes place, the large protein enthalpy in pR_2 ensures the transformation to pB.

Spectrally silent intermediate species

Using low temperature trapping methods, many intermediate species have been identified (Imamoto et al., 1996). At room temperature, the reaction scheme was considered to be simple, and only four species have been reported from picosecond to second time range. Although a branched scheme before the creation of pR was recently proposed even at room temperature (Imamoto et al., 2001b), it is considered to be still correct that only one species exists after 20 ns from the photo-excitation. In these studies, the optical transitions of the chromophore have been used to study the kinetics and to identify the intermediate species. This traditional technique has been applied not only to PYP but also to most biological photosensors. However, intermediate species having a different protein structure far from the chromophore could participate in the reaction, and it is important to find such spectrally silent intermediate species to elucidate the reaction mechanism. In fact, in the photoreaction sequence of the octopus rhodopsin, Nishioku et al. (2001) have found a new intermediate species that could not be detected by using the optical transition of the chromophore, retinal, and it could be a key intermediate to activate the G-protein. In the present study, we observed a new kinetics that cannot be detected by the optical transitions of the chromophore in the PYP photocycle. This kinetics is attributed to protein movements distant from the chromophore.

The structural changes on the femtosecond time scale are probably restricted to the chromophore itself within the closely packed hydrophobic binding pocket. The twist of the thiol ester bond facilitates the completion of the chromophore *trans-cis* isomerization and as a consequence of this, the protein environment around the chromophore undergoes conformational changes to produce pR_1. After this event, the protein structure distant from the chromophore changes, i.e., $pR_1 \rightarrow pR_2$, which must be triggered by the

isomerization. Because the thermal grating component for this $pR_1 \rightarrow pR_2$ process is not large, the energy is not so much stabilized during this process. Moreover, considering a moderate magnitude of the volume change (Table 3), we think that the entropy change is the main factor driving this process. The chromophore breaks its H-bonds to Tyr-42 and Glu-46 and Arg-52 moves to pick up a proton to complete the $pR_2 \rightarrow pB$ process (Xie et al., 2001; Brudler et al., 2001).

We do not know exactly how many residues are participated in the protein structural change of $pR_1 \rightarrow pR_2$. However, if we notice that every mutation in this study including replacement of Trp-119 that is located rather far distance from the chromophore site changes the magnitude of the slow dynamics (ΔV for $pR_1 \rightarrow pR_2$), we may speculate that a considerable number of residues are moving during this process. This movement may cause the loosened structure of the protein part of pR_2 as suggested by the values of $\Delta\alpha$.

Recently, time-resolved Fourier transform infrared (FTIR) studies of PYP revealed some interesting structural changes at room temperature (Xie et al., 2001; Brudler et al., 2001). The infrared difference spectrum between pG and pR clearly showed the presence of the hydrogen bond between Glu-46 and the chromophore. After deprotonation of Glu-46 ($pR_2 \rightarrow pB$), a prominent global structure change was observed in the amide I band. Our observed spectral silent structure change $pR_1 \rightarrow pR_2$ was not observed in their time-resolved FTIR spectra, probably because this structural change does not change the infrared spectrum in the amide I band.

Structural change of PYP

In the previous papers, we reported the temperature-dependent volume change of $pG \rightarrow pR_2$ of WT-PYP, and this dependence has been attributed to the different thermal expansion coefficient, $\Delta\alpha$, between pG and pR_2 (Takeshita et al., 2000, 2002). A thermodynamical relationship indicates that α is proportional to the cross-correlation of the volume (V) and entropy (S) fluctuations (Heremans and Smeller, 1998),

$$\langle SV - \langle S\rangle\langle V\rangle\rangle = kTV\alpha$$

in which $< >$ indicates the ensemble average, and k is the Boltzmann factor. A large α means a large structural and/or entropy fluctuation. Considering that no large global structure change was observed by the time-resolved FTIR in the amide I region in the pR_2 state (Xie et al., 2001; Brudler et al., 2001), we think that the larger α for pR_2 than for pG reflects a softer conformation in the pR_2 state than in the pG state with a similar equilibrium conformation. It is reasonable to speculate that this larger conformational flexibility in pR_2 causes the subsequent larger protein structural change in the next $pR_2 \rightarrow pB$ process. A similar temperature dependence of ΔV is observed for all three mutants we studied here. The magnitude of $\Delta\alpha$ is also very similar. This observation is consistent with the softness of the global conformation, because the replacement of one residue should not affect the global change of the protein structure significantly as long as the photocyclic reaction takes place.

Another physical property sensitive to the global structural change is the diffusion coefficient. D can probe the average dimension of the protein, and a small D for pB should be a result of a large global structure change in the $pR_2 \rightarrow pB$ process. The similar D of pB for the WT-PYP and the mutants are also consistent with the expectation that the replacement of one residue does not change the global feature. If D is taken as the indicator of the compact factor by the reaction, we can say that the compact factor does not change by these site-directed mutations.

Contrary to $\Delta\alpha$ and D, ΔV for the $pR_1 \rightarrow pR_2$ process is sensitive to the mutation (Table 3). This position sensitive ΔV indicates that ΔV reflects a more local change of the protein than $\Delta\alpha$ and D.

SUMMARY

To obtain information of the structural dynamics of PYP, TG method was applied to the three PYP mutants, R52Q, P68A, and W119G. Interestingly, we observed a new dynamics on microsecond time scale that has never been detected by other spectroscopic methods so far. Because pR is already created on this time scale, this new dynamics indicates that the protein structure far from the chromophore is still moving after the pR state is created. Therefore, the pR state is not a single state, but subsequent change of the protein structure distant from the chromophore is essential to prepare pR leading to pB; that is, the protein structure around the chromophore is initially changed within 3 ns and then the other protein part moves with a microsecond lifetime. The kinetics and ΔV for the $pR_1 \rightarrow pR_2$ process are sensitive to the mutations, whereas $\Delta\alpha$ and D are not much influenced. This suggests that ΔV reflects the local character of the residues, whereas $\Delta\alpha$ and D reflect more global structural change, which should not be changed so much by the replacement of a single amino acid residue.

REFERENCES

Baca, M., G. E. O. Borgstahl, M. Boissinot, P. M. Burke, D. R. Williams, K. A. Slater, and E. D. Getzoff. 1994. Complete chemical structure of photoactive yellow protein: novel thioester-linked 4-hydroxycinnamyl chromophore and photocycle chemistry. *Biochemistry.* 33: 14369–14377.

Borgstohl, G. E. O., D. R. Williams, and E. D. Getzoff. 1995. 1.4 Å structure of photoactive yellow protein, a cytosolic photoreceptor: unusual fold, active site, and chromophore. *Biochemistry.* 34:6278–6287.

Braslavsky, S. E., and G. E. Heibel. 1992. Time-resolved photothermal and photoacoustic methods applied to photoinduced processes in solution. *Chem. Rev.* 92:1381–1410.

Brudler, R., R. Rammelsberg, T. T. Woo, E. D. Getzoff, and K. Gerwert. 2001. Structure of the I1 early intermediate of photoactive yellow protein by FTIR spectroscopy. *Nat. Struct. Biol.* 8:265–270.

Craven, C. J., N. M. Derix, J. Hendriks, R. Boelens, K. J. Hellingwelf, and R. Kaptein. 2000. Probing the nature of the blue-shifted intermediate of photoactive yellow protein in solution by NMR: hydrogen-deuterium exchange data and pH studies. *Biochemistry.* 39:14392–14399.

Devanathan, S., A. Pacheco, L. Ujj, M. Cusanovich, G. Tollin, S. Lin, and N. Woodbury. 1999. Femtosecond spectroscopic observation of initial intermediates in the photocycle of the photoactive yellow protein from *Ectothiorhodospira halophila. Biophys. J.* 77:1017–1023.

Düx, P., G. Rubinstenn, G. W. Vuister, R. Boelens, F. A. A. Mulder, K. Hård, W. D. Hoff, A. R. Kroon, W. Crielaard, K. J. Hellingwerf, and R. Kaptein. 1998. Solution structure and backbone dynamics of the photoactive yellow protein. *Biochemistry.* 37:12689–12699.

Genick, U. K., G. E. O. Borgstahl, K. Ng, Z. Ren, C. Pradervand, P. M. Burke, V. ärajer, T. Teng, W. Schildkamp, D. E. McRee, K. Moffat, and E. D. Getzoff. 1997a. Structure of a protein photocycle intermediate by millisecond time-resolved crystallography. *Science.* 275:1471–1475.

Genick, U. K., S. Devanathan, T. E. Meyer, I. L. Canestrelli, E. Williams, M. A. Cusanovich, G. Tollin, and E. D. Getzoff. 1997b. Active site mutants implicate key residues for control of color and light cycle kinetics of photoactive yellow protein. *Biochemistry.* 36:8–14.

Heremans, K., and L. Smeller. 1998. Protein structure and dynamics at high pressure. *Biochim. Biophys. Acta.* 1386:353.

Hoff, W. D., P. Düx, K. Hård, B. Devreese, I. M. Nugteren-Roodzant, W. Crielaard, R. Boelens, R. Kaptein, J. van Beeumen, and K. J. Hellingwerf. 1994a. Thioester-linked p-coumaric acid as a new photoactive prosthetic group in a protein with rhodopsin-like photochemistry. *Biochemistry.* 33:13959–13962.

Hoff, W. D., I. H. M. van Stokkum, H. J. van Ramesdonk, M. E. van Brederode, A. M. Brouwer, J. C. Fitch, Meyer, T. E., R. van Grondelle, and K. J. Hellingwerf. 1994b. Measurement and global analysis of the absorbance changes in the photocycle of the photoactive yellow protein from *Ectothiorhodospira halophila. Biophys. J.* 67:1691–1705.

Imamoto, Y., M. Kataoka, and F. Tokunaga. 1996. Photoreaction cycle of photoactive yellow protein from *Ectothiorhodospira halophila* studied by low-temperature spectroscopy. *Biochemistry.* 35:14047–14053.

Imamoto, Y., H. Koshimizu, K. Mihara, O. Hisatomi, T. Mizukami, K. Tsujimoto, M. Kataoka, and F. Tokunaga. 2001a. Roles of amino acid residues near the chromophore of photoactive yellow protein. *Biochemistry.* 40:4679–4685.

Imamoto, Y., M. Kataoka, and F. Tokunaga, T. Asahi, and H. Masauhara. 2001b. Primary photoreaction of photoactive yellow protein studied by subpicosecond-nanosecond spectroscopy. *Biochemistry.* 40:6047–6052.

Kandori, H., T. Iwata, J. Hendriks, A. Maeda, and K. J. Hellingwerf. 2000. Water structural changes involved in the activation process of photoactive yellow protein. *Biochemistry.* 39:7902–7909.

Koh, M., G. van Driessche, B. Samyn, W. D. Hoff, T. E. Meyer, M. A. Cussanovich, and J. J. van Beeumen. 1996. Sequence evidence for strong conservation of the photoactive yellow proteins from the halophilic bacteria *Chromatium salexigens* and *Rhodospirillum salexigens. Biochemistry.* 35:2526–2534.

Meyer, T. E. 1985. Isolation and characterization of soluble cytochromes, ferredoxins and other chromophoric proteins from the halophilic phototrophic bacterium *Ectothiorhodospira halophila. Biochem. Biophys. Acta.* 806:175–183.

Mihara, K., O. Hisatomi, Y. Imamoto, M. Kataoka, and F. Tokunaga. 1997. Functional expression and site-directed mutagenesis of photoactive yellow protein. *J. Biochem.* 121:876–880.

Nishioku, Y., M. Nakagawa, M. Tsuda, and M. Terazima. 2001. A spectrally silent transformation in the photolysis of octopus rhodopsin: a protein conformational change without any accompanying change of chromophore's absorption. *Biophys. J.* 80:2922–2927.

Ohishi, S., N. Shimizu, K. Mihara, Y. Imamoto, and M. Kataoka. 2001. Light induces destabilization of photoactive yellow protein. *Biochemistry.* 40:2854–2859.

Rubinstenn, G., G. W. Vuister, F. A. A. Mulder, P. Düx, R. Boelens, K. J. Hellingwerf, and R. Kaptein. 1998. Structure and dynamic change of photoactive yellow protein during its photocycle in solution. *Nat. Struct. Biol.* 5:568–570.

Takeshita, K., N. Hirota, Y. Imamoto, M. Kataoka, F. Tokunaga, and M. Terazima, 2000. Temperature-dependent volume change of the initial step of the photoreaction of photoactive yellow protein (PYP) studied by transient grating. *J. Am. Chem. Soc.* 122:8524–8528.

Takeshita, K., Y. Imamoto, M. Kataoka, F. Tokunaga, and M. Terazima, 2002. Themodynamical and transport properties of intermediate states of photo-cyclic reaction of photoactive yellow protein. *Biochemistry.* 41: 3037–3048.

Terazima, M., and N. Hirota. 1993. Translational diffusion of a transient radical studied by the transient radical studied by the transient grating method, pyrazinyl radical in 2-propanol. *J. Chem. Phys.* 98:6257–6262.

Terazima, M. 1998. Photothermal studies of photophysical and photochemical processes by the transient grating method. *Adv. Photochem.* 24: 255–338.

Ujj, L., S. Devanathan, T. E. Meyer, M. A. Cusanovich, G. Tollin, and G. H. Atkinson. 1998. New photocycle intermediates in the photocycle yellow protein from *Ectothiorhodospira halophila*: picosecond transient absorption spectroscopy. *Biophys. J.* 75:406–412.

Van Brederode, M. E., T. Gensch, W. D. Hoff, K. J. Hellingwerf, and S. E. Braslavsky. 1995. Photoinduced volume change and energy storage associated with the early transformation of the photoactive yellow protein from *Ectothiorhodospira halophila. Biophys. J.* 68:1101–1109.

Van Brederode, M. E., W. D. Hoff, I. H. M. van Stokkum, M. Groot, and K. J. Hellingwerf. 1996. Protein folding thermodynamics applied to the photocycle of the photoactive yellow protein. *Biophys. J.* 71:365–380.

Xie, A., L. Kelemen, J. Hendriks, B. J. White, K. J. Hellingwerf, and W. D. Hoff. 2001. Formation of a new buried charge drives a large-amplitude protein quake in photoreceptor activation. *Biochemistry.* 40:1510–1517.